

Search for nuclear excitation by electronic transition in ^{235}U G. Claverie, M. M. Aléonard,* J. F. Chemin, F. Gobet, F. Hannachi, M. R. Harston, G. Malka, and J. N. Scheurer
Centre d'Etudes Nucléaires de Bordeaux-Gradignan, 33175 Gradignan, France

P. Morel and V. Méot

CEA/Service de Physique Nucléaire, B.P.12, 91680, Bruyères le Châtel, France

(Received 16 February 2004; published 6 October 2004)

We have searched for the nuclear excitation by electronic transition (NEET) of the isomeric level at 76 eV in ^{235}U in a plasma induced by a YAG laser with an energy of 1 Joule and a full width at half maximum time distribution of 5 ns, operating at an intensity of 10^{13} W cm^{-2} . We present a thorough description of the experimental conditions and analysis of our data. In this experimental situation we do not detect any excitation of the isomeric level, a result that is at variance with a previously reported one. An upper limit of 6×10^{-6} per atom and per second averaged over the laser-pulse width has been set on the nuclear excitation rate. This value is compared with results obtained in previous experimental and theoretical works.

DOI: 10.1103/PhysRevC.70.044303

PACS number(s): 23.90.+w, 27.90.+b

I. INTRODUCTION

The excitation of nuclear levels induced by the transfer of energy from the atomic part to the nuclear part of an atom has been the subject of a large number of investigations. The aim underlying this research is the possibility of finding an efficient mechanism to excite nuclear isomers in view of further applications for energy storage and development of lasers based on nuclear transitions. This process called NEET, for nuclear excitation by electronic transition, was first suggested by Morita to explain the excitation of a level at approximately 43 keV in ^{235}U [1]. Morita has pointed out the resonant character of the energy exchange process. It requires the existence in the same atom (or ion) of two atomic states with an energy difference that lies very close to the energy difference between two nuclear states. The idea was later applied to the excitation of other low-energy levels in a variety of nuclei. The best known low-energy transitions that have been considered are the transitions at 77.3 keV, 69.5 keV, and 102.9 keV, respectively in the nuclei ^{197}Au [2], ^{189}Os [3], and ^{237}Np [4]. However, initially very contradictory results were obtained for the NEET process probability in these nuclei [5]. In general, the experimental approach was based on the photoexcitation of the atomic core by a strong external source of photons followed by the observation of the characteristic radiation emitted in the deexcitation of the nuclear level. The discrimination between the incident radiation and the nuclear deexcitation radiation was based on the specific characters of the nuclear transition which is monochromatic, and delayed in time with a delay characteristic of the half-life of the nuclear level. Recently, Kishimoto *et al.* have performed a measurement of the NEET excitation probability of the 77 keV level in ^{197}Au using the pulsed light beam of a synchrotron radiation facility [2]. This very convincing result is in agreement with recent theoretical predictions [5].

In this context, several experiments have been carried out over the last 30 years to observe the excitation of the extremely low-energy nuclear level at 76 eV in ^{235}U using a pulsed high intensity laser beam. In these experiments, the plasma generated in the interaction of the laser with the U target was collected on a catcher foil subsequently placed in front of an electron multiplier. The excitation of the nuclear isomeric level was detected by means of the internal conversion (IC) electrons emitted in its decay. The results show significant differences. Using a 1 Joule, 100 ns CO_2 laser and a target of natural uranium, Izawa *et al.* [6] observed a strong signal of delayed low-energy electrons, attributed to the decay of the 76 eV level after excitation by a NEET process. Goldansky and Namiot [7] suggested that in these experimental conditions the excitation probability by NEET should be negligible and they proposed an interpretation of the results in terms of NEEC. NEEC is the excitation of the nucleus by the capture of a free electron into a bound orbital. The energy gained by the system can be resonantly transferred to the nucleus. The associated probability for this excitation mechanism in the case of the 76 eV level in ^{235}U has been discussed in Ref. [8]. Arutynyan *et al.* have attempted a similar experiment with a CO_2 laser (5 J, 200 ns) and a 6% enriched ^{235}U ceramic target but failed to observe the excitation of the isomeric state [9]. In a second experiment, the same group observed the excitation of the isomeric state detected in a plasma induced by a high intensity beam of 500 keV electrons. The temperature of the plasma was of the order of 20 eV. It was shown in [8] that this positive result was most likely due to direct excitation of the U nuclei by inelastic electron scattering from the incident beam rather than to a NEET or a NEEC mechanism. In fact, it is very difficult to compare these results because of the lack of details concerning the experimental conditions such as laser-beam focusing, diagnostics of the plasma temperature, number of collected atoms on the catcher foil, thickness of the U layer, electron detection efficiency, or parasitic electron emission phenomena. Finally, a more recent attempt to excite the isomeric level in ^{235}U by Bounds and Dyer [10] deserves

*Corresponding author. Electronic address:
aleonard@cenbg.in2p3.fr

to be mentioned. In this case, a low-energy CO₂ laser interacting with a 93% enriched U target generated a U vapor which was illuminated by a picosecond (ps) laser to create a plasma. The intensity of the ps laser beam, ranging between 10¹³ and 10¹⁵ W cm⁻², was deduced from a measurement of the charge state distribution of the U ions in the plasma. The U ions were deposited on a plate and their delayed electron emission was analyzed. An electric field permitted the separation between neutral and ionized U species. A time-of-flight measurement of the collected U ions provided a crude estimate of the number of ions in charge states ranging between 1⁺ and 5⁺. In the paper, the delayed emission of exo-electrons by the collector was mentioned and this contribution was subtracted off before setting the limit on the nuclear excitation rate. Problems related with the short mean-free path of the low-energy IC electrons in the catcher foil or in the deposited U layer were also considered. No excitation of the isomeric level was observed in the experiment.

In this paper, we report the result of an experiment searching for the nuclear excitation of the 76 eV isomeric level in ²³⁵U in a plasma induced by a laser. We used a 1 J, 5 ns, Nd-YAG laser, at a wavelength of 1.06 μm and targets 93% enriched in ²³⁵U. In Sec. II, we present the interest in searching for the NEET process in a plasma induced by laser and we give the main characteristics of this plasma. In Sec. III, we review the main difficulties encountered in this type of experiment. Finally, we give our upper limit for the excitation rate of the isomeric level and we compare it with other results and the recent theoretical predictions of Refs. [8,11].

II. NEET IN A PLASMA INDUCED BY LASER

The NEET process is the inverse of the nuclear internal conversion between two bound atomic states (BIC) which has been recently demonstrated in ¹²⁵Te [12]. BIC is a resonant process as is NEET. In the Te case it was shown that the energy matching between the atomic-energy transition and the nuclear-energy transition was possible because the spacing between the atomic levels is dependent on the charge state and on the atomic configuration within each charge state [13]. The interest for searching for the NEET process in a plasma induced by a laser follows the idea that the energy matching can be reached by tuning the atomic-energy transition by varying the ionic charge state. The laser beam is not used to directly excite the nuclear level by some multiphotonic process, but to create a dense and hot plasma of U matter. In the plasma, U atoms are ionized and have a charge state distribution with a mean-value dependent on the local plasma temperature and density. Furthermore, for each of the charge states, the U ions can have many configurations corresponding to the various arrangements of electrons in atomic shells and to the different couplings between the electron spins. Each atomic configuration corresponds to a particular set of atomic energies. Some configurations may have transitions which match more or less closely the energy of the nuclear transition between the ground state and the first excited state in ²³⁵U. The nucleus can absorb the virtual photon emitted in the atomic transition only if the energy mismatch between the two transition energies is of the order of

the width of the system. Due to electrons-ion collisions in the hot plasma, the widths of the excited atomic levels are strongly increased. For example, the natural width of a 5d hole in the U atom is of the order of 10⁻⁵ eV. In a plasma at a temperature of 100 eV, this width becomes dominated by the Stark broadening or collisional effects and reaches a value as large as 20 meV for an electronic density of about 6 × 10²⁰ cm⁻³. The widths are strongly dependent on the local density and temperature of the electrons in the plasma. This greatly enhances the probability of matching between the atomic and the nuclear transition energies.

The theory of NEET in a plasma has been developed in [8,11,14]. In a recent paper, Morel *et al.* [11] have considered, in a microscopic formalism, the time evolution of the coupling between the nucleus and its electronic environment leading to a time-dependent probability of NEET, $P(t)$. It was demonstrated that $P(t)$ will reach the asymptotic value valid for large values of t already derived in [14] if the characteristic time of $P(t)$ given by the widths of the atomic configurations is smaller than the duration of the plasma local equilibrium. Under this condition, atomic level populations can be considered as stationary as compared to the plasma dynamic. In the range of temperatures and densities generated by a laser at intensities of the order of 10¹³ W cm⁻², coupled hydrodynamic and atomic calculations (see below) show that in the regions of interest the atomic widths always meet this requirement due to electron collisions and Stark broadening effects [11]. As a consequence, the asymptotic form of $P(t)$ can be used in the following.

Assuming a U ion, with a charge state q , in an atomic state i under plasma conditions described by an electron density n_e and a temperature T , the NEET probability can be written as

$$P^{q,i,f} = (1 + \Gamma_f/\Gamma_i)[V_{if}^2/(\delta_{if}^2 + (1/4)(\Gamma_i + \Gamma_f)^2)], \quad (1)$$

where V_{if} is the matrix element between the initial and the final atomic-nuclear states, Γ_i , Γ_f are the widths of the initial and final atomic-nuclear state, and δ_{if} is the energy mismatch between the atomic and the nuclear transitions. From $P^{q,i,f}$ we can define λ_{neet} , the rate for nuclear excitation of the U nucleus in a plasma:

$$\lambda_{neet} = \sum_q \sum_{i,f} R^{q,i}(n_e, T) \lambda^{q,i,f}(n_e, T) P^{q,i,f}, \quad (2)$$

where $R^{q,i}(n_e, T)$ is the probability to find a U ion in the charge state q and atomic state i and $\lambda^{q,i,f}(n_e, T)$ is the decay rate of the atomic state i to a final atomic state f . $\lambda^{q,i,f}$ depends on the plasma conditions. λ_{neet} is a very convenient quantity for comparison with the experimental results. The number of nuclei excited by NEET in a plasma induced by a laser with a pulse duration τ is related to the total number of ions in the plasma, N_{at} , by the relation:

$$N_{neet} = \int_0^\tau N_{at}(t) \lambda_{neet}(t) dt. \quad (3)$$

In ²³⁵U the nuclear transition between the ground state and the first excited state [$E_n = (76.8 \pm 0.8)$ eV] is of E3 character [15]. The half-life of the $J^\pi = 1/2^+$ excited level is 26.8 min and depends slightly on the chemical state of the U [16].

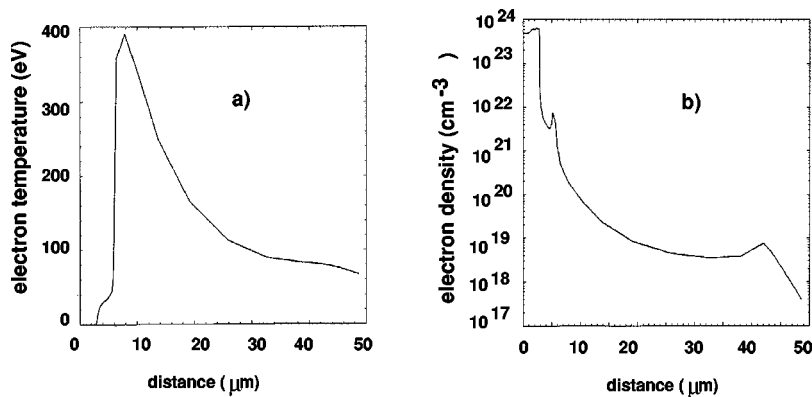


FIG. 1. (a) electronic temperature and (b) density profiles at the maximum laser intensity on the U target (distance relative to the target surface).

The IC coefficient is very large ($\sim 10^{20}$) but has never been measured precisely. In spite of these uncertainties it has been shown [8] that the atomic transitions $6p_{1/2}-5d_{5/2}$ in U^{10+} ions and $6d_{5/2}-6p_{1/2}$ in U^{23+} ions have energies nearly equal to E_n . Owing to combined uncertainties on E_n and on the calculated atomic energies leading to an energy mismatch of 4 eV, theoretical values of λ_{neet} range between 10^{-9} and 10^{-5} s^{-1} for the $6p_{1/2}-5d_{5/2}$ group of transitions and between 10^{-5} and 10^{-1} for the $6d_{5/2}-6p_{1/2}$ group of transitions. Analytical relations between the laser intensity I , T and the effective charge state q can be obtained in the framework of some simplified hydrodynamic models of a plasma [17]. In these models, the laser radiation intensity is absorbed in a thin layer of plasma where the electron density corresponds to the cut-off density (or critical density, n_c) at the laser wavelength, $n_e = n_c = 10^{21} \text{ cm}^{-3}$. Local equilibrium is assumed considering that the laser energy is dissipated by dynamical plasma expansion and ionization of the matter. The plasma is supposed to expand in a direction normal to the target without any growth in lateral directions. In these simplified models T and q are given by:

$$T(\text{eV}) \approx 5.2 \times 10^6 A^{0.2} (I\lambda)^2, \quad (4)$$

$$q \approx 0.66(AT)^{0.33}, \quad (5)$$

where $A=235$ for U plasma. From these simple relations one gets a very crude estimate of the minimum limit of effective laser intensities required on the target to obtain the charge state values $q=10$ and $q=23$. The time dependence of the laser pulse is not taken into account and the radiation emission escaping from the plasma is neglected, both effects add together to lower the plasma temperature. Including a radiative recombination term and using a Gaussian time distribution for the laser intensity characterized by a pulse half-width of 5 ns, the model shows that the plasma will reach a maximum temperature around 260 eV, 12 ns after the start of the laser pulse for a laser intensity of $5 \times 10^{12} \text{ W cm}^{-2}$ [17]. This maximum temperature decreases if one takes into account a lateral expansion of the plasma in a three-dimensional model and also the effect of the opacity on the radiation emission. Finally, the maximum value can only be seen as an estimate in a very thin layer of the plasma at the critical density.

In order to improve our knowledge of the dynamics of the plasma, we performed hydrodynamic bi-dimensional calcu-

lations of the plasma expansion. The laser ene radiation dependent ionization model proposed by Busquet [18]. It takes into account the nonlocal thermodynamic equilibrium effects present during the plasma expansion. Moreover, in the radiative intensity transport equations a coupling term links the radiative and the electronic equations to reproduce the photon absorption and emission in matter. The electron heat flux is calculated using the heat conductivity given by Spitzer [19].

The present calculations correspond to a laser intensity following a Gaussian temporal shape characterized by a pulse half-width of 5 ns and a peak intensity of $10^{13} \text{ W cm}^{-2}$ with a full width at half maximum focal spot of 50 μm . Laser matter interaction occurs deeper and deeper until the critical density is reached. The target is divided in a finite number of cells. The code follows the behavior of the matter in the cells during the time of interaction with the laser. The variation of the plasma electronic temperature and density with respect to the target distance are respectively given in Figs. 1(a) and 1(b) at the time of maximum laser intensity. At a given time, one may roughly define three regions in the plasma. Near the target we find a dense and cold region heated by electron conductivity and hard X-rays from the conversion region. In this so-called absorption-reemission region the temperature evolves slowly between 15 and 30 eV. This region can be considered as being in a local thermodynamic equilibrium (LTE). Next comes the conversion layer characterized by steep gradients of temperature and density where the laser energy is deposited once the critical density is reached. The properties of this region roughly correspond to the characteristics given by the simplified model mentioned above. The temperature at the maximum intensity of the laser pulse reaches 400 eV in this bi-dimensional approximation. Finally, in front of the critical density region we have a region of decreasing density and temperature. The characteristic lengths of the three regions at a time $t=5$ ns are respectively of the order of 60 μm , 100 μm , and 0.5 mm. Figure 2 shows the variation of the mean-charge state of the U ions in a typical cell of matter versus the irradiation time. At the beginning, the atoms are heated by electron conduction. Around 5 ns, the cell density reaches the critical density and the laser deposits its energy directly in the cell. The temperature rises suddenly and the density drops. Thereafter, the cell is no longer heated and the temperature gradually decreases. One sees on the figure that the laser beam conditions allow

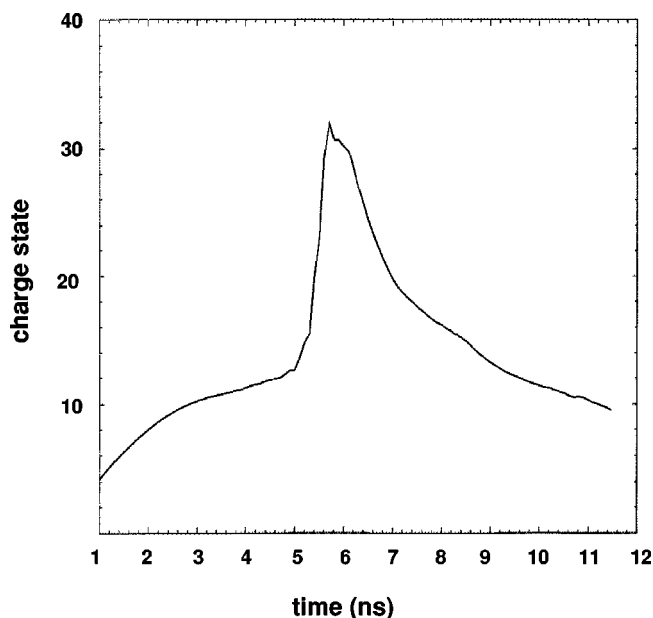


FIG. 2. U charge state dependence on the laser-matter interaction time.

the population of U in the 23^+ charge state in the absorption region but the U density is rather low and the ions remain in this condition only for a short time. The conditions for populating U in the 10^+ charge state seem better both in the absorption-reemission region where the ion density is high and in the large fraction of the plasma volume behind the absorption region. These calculations clearly show that the NEET rate strongly depends on the dynamics of the plasma during the laser pulse.

Morel *et al.* [11] have coupled a hydrodynamic code describing the evolution of the plasma induced by the laser with a multiconfiguration atomic code in order to obtain a reliable theoretical mean value of the NEET rate of the 76 eV level of ^{235}U as a function of T and ρ . In this calculation, it is assumed that the plasma is at LTE. The two favorable zones for the NEET, corresponding to the $6p_{1/2}-5d_{5/2}$ group of transitions at T around 20 eV and to the $6d_{5/2}-6p_{1/2}$ group of transitions at T around 100 eV, are clearly shown in the results of these calculations. For example, at an ionic density of 1 g cm^{-3} the NEET rate evolves from 10^{-6} s^{-1} to $2 \times 10^{-4} \text{ s}^{-1}$ depending on the temperature. As mentioned before, the LTE condition is met in the experiment in the absorption-reemission zone in which NEET excitation proceeds via the $6p_{1/2}-5d_{5/2}$ group of transitions.

III. EXPERIMENTAL METHOD AND SET-UP

The experimental method used in the present paper follows the general basic approach of the previous measurements. In a first step, a U plasma is formed by interaction of a laser beam with a U target. The plasma expands in vacuum and the U atoms are collected on a catcher foil. In a second step, the catcher foil is moved in front of an electron detector to search for the decay by internal conversion of the level at 76 eV in ^{235}U , called hereafter $^{235}\text{U}^m$, possibly excited in the

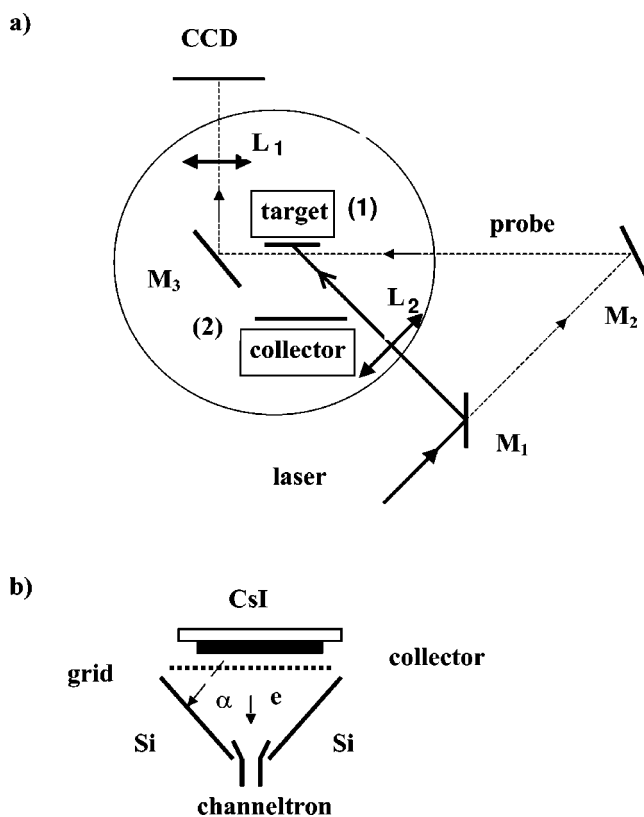


FIG. 3. (a) Schematic drawing of the irradiation set-up. L1 and L2 are lenses, M1, M2, M3 mirrors. The difference in the path lengths between the main and the probe beams is adjustable by moving M2. The target and the collector are respectively mounted on the supports (1) and (2) which can be moved separately. At the end of the irradiation, the support (2) is automatically transferred to the detection chamber. (b) Schematic drawing of the detection set-up installed under vacuum in a chamber not represented on the drawing. The collector and the CsI detector are mounted on the same support. The collector is biased at 2 V. The thin dashed line represents a grid biased at 175 V. Two out of the four Si detectors are represented, they are mounted symmetrically with respect to the electron multiplier labeled channeltron. The other extremity of the channeltron, not represented here, is biased at 2800 V.

plasma by a NEET process. The nuclear excitation is signaled by the detection of electrons with a maximum energy of the order of 60 eV corresponding to the nuclear transition energy minus the binding energy of the converted electron in the $6d$ shell [20]. The number of electrons emitted versus the time elapsed after the end of the irradiation must follow an exponential law with a half-life equal to 26.8 min.

The experimental set-up, used to create and to characterize the plasma in the laser-target interaction is given in Fig. 3. A 1 Joule Nd-YAG laser beam was focused onto 50 μm thick uranium targets. The time distribution of the laser pulses was Gaussian with a full width at half maximum of 5 ns. The targets were metallic 93% enriched ^{235}U foils. For comparison, we also used targets of natural U in which the concentration in ^{235}U was only 0.5%. The laser beam was focused on the target with an $f/10$ lens installed inside the vacuum chamber. The angle between the laser beam and the target surface was 45 deg. Under these conditions 80% of the

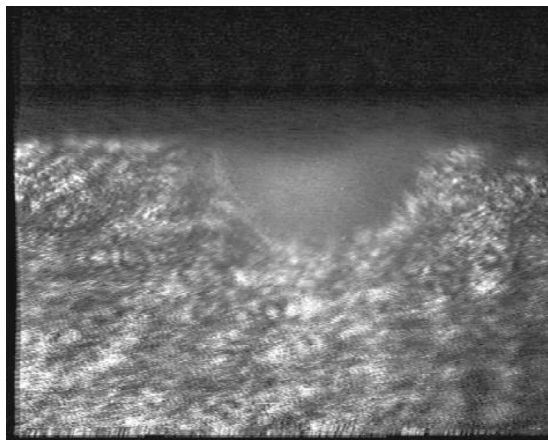


FIG. 4. Image of the plasma taken with the set-up shown in Fig. 3(a). The black and plane part of the image is given by the target support. The curved gray part corresponds to the plasma. The delay between the main and the probe beams is 5 ns. In a direction normal to the target support the extension of the plasma is 100 μm .

laser energy was found in a 50 μm diameter spot leading to a laser intensity, I , of the order of $10^{13} \text{ W cm}^{-2}$. For data-taking we used a shot-by-shot mode of operation. After each shot the target was automatically translated by 200 μm so that the next laser pulse hit a clean area of the target. The U plasma expands into the vacuum in a direction normal to the target surface. The dimensions of the plasma were checked by ombrography. For this purpose, a small fraction of the initial laser beam was set apart to serve as a probe beam. This probe beam was delayed with respect to the main beam and reached the interaction area in a direction parallel to the target surface. The light refracted by the plasma was used to create an image of the dense part of the plasma (where $n_e \geq n_c$) in a CCD camera. An example of such an image, taken with a 5 ns delay between the main and the probe beams, is shown in Fig. 4. In this case the target was a 50 μm thick gold foil and the dimension of the dense region was of the order of 100 μm .

The velocity distribution of ion at the end of the laser pulse was measured in a time of flight charge collector device placed at a distance of 6.2 cm from the target. The collected charged particles, electrons and ions, generated a current in the collector which was analyzed with a digital oscilloscope. The electrons, which move much faster than the ions, produce a well-defined start signal in the device. The ions induce a broad peak reflecting the dispersion of the ion velocities in the plasma. The delay between the electron signal and the maximum of the broad distribution gives an estimate of the ion velocity C_s . One finds $C_s = (7 \pm 1)10^6 \text{ cm s}^{-1}$. In the simple stationary model of plasma described previously C_s is related to the temperature. One obtains $T = (400 \pm 90) \text{ eV}$.

The U target and the collector were set parallel to each other at a distance of 5 cm. Several collectors have been tested. For reasons given later we finally adopted self-supporting 2 μm thick gold foils. The area for plasma collection was limited to 5.76 cm^2 by a square-shaped aperture positioned in front of the collector. After irradiation of the U

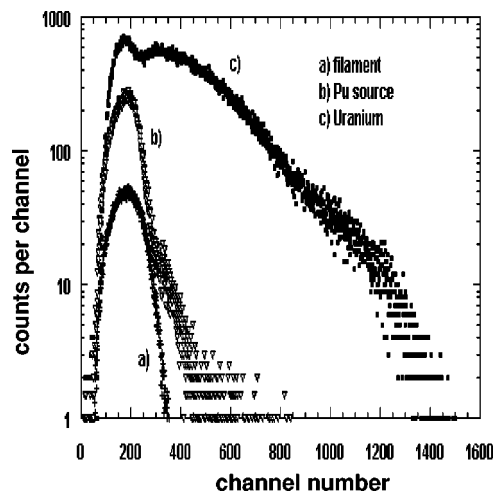


FIG. 5. Pulse-height distribution of the signals issued from the electron detector. (a) the electron source is a lamp filament, data points are divided by 30; (b) the electrons are emitted from $^{235}\text{U}^m$ implanted in a thin gold foil, the data points are divided by 3; (c) the electron source is a layer of ^{235}U deposited with the laser on a thin gold foil.

targets with the laser beam, the collector was automatically transferred to the detection chamber in order to analyze the nuclear decay by IC of the U atoms deposited on the collector. The time needed for the transfer was typically 90 s. The vacuum levels in the irradiation and the detection chambers were different. In the detection chamber the vacuum was kept below 5×10^{-7} torr. A schematic drawing of the detection set-up is given in Fig. 3(b). The delayed electrons were detected in an electron multiplier [21] having an aperture diameter of 1.6 cm. The channeltron was mounted 5 cm away from the collector surface. The head of the channeltron was biased at 200 V with respect to ground. The voltage across the channeltron was 2600 V. An electrostatic grid, biased at 175 V, was installed between the collector and the channeltron head. In these operating conditions the electron multiplication factor was almost independent of the electron energy. The channeltron signal was sent to a spectroscopic amplifier feeding the input of an ADC, and to a fast amplifier followed by a constant fraction discriminator (CFD). The output of the CFD was used to trigger the acquisition.

IV. CHARACTERISTICS OF THE ELECTRON DETECTION

The pulse-height distribution (PHD) of the channeltron signals is given in Fig. 5 for three different situations. The first curve labeled (a) is obtained from a lamp filament mounted in place of the collector. Electrons emitted with a thermal energy distribution produce a pulse distribution which presents a single peak. The full width at half maximum of the distribution agrees with the expected 50% resolution of the channeltron. In the second case [Fig. 5(b)] the electrons are emitted from the IC decay of $^{235}\text{U}^m$ implanted in a thin gold foil (U atoms in the isomeric state are produced in the alpha decay of ^{239}Pu). The use and the charac-

teristic of the ^{239}Pu source are detailed in the appendix. The PHD of the channeltron pulses in this case, shown in curve b, has the same shape as curve a. Finally, curve c shows the PHD recorded after deposition of the U plasma on a thin gold collecting foil. Curve c is very different from curves a and b. The low amplitude part of the PHD shows a peak with a shape identical to the ones observed in curves a and b but the high amplitude part presents a broad structure which is absent or negligible in the preceding conditions. Since the electron multiplier is biased in a saturated mode, the PHD does not depend on the electron energy as shown by comparing curves a and b. Nevertheless, if n electrons arrive simultaneously in the detector, the output signal will be n times larger than the signal produced by a single electron. This structure is explained by the emission of alpha particles coming from the radioactive uranium nuclei deposited on the collector. The α particles are emitted isotropically in the layer with an initial energy of the order of 5 MeV. Depending on the emission direction, the particles are slowed down in the Au backing or in the U layer, generating a large number of free delta electrons with a wide energy distribution which can escape from the target after multicollisional processes. The electron multiplicity will depend on the direction of emission, and on the U layer and backing thicknesses. The isotopic concentration of uranium on the collector reproduces the isotopic composition of the target, i.e., 93.2% ^{235}U , 0.8% ^{234}U , and 5.76% ^{238}U . The half-life of ^{234}U is only 2.45×10^5 years, much shorter than the half-lives of the 235 and 238 isotopes. Consequently, in spite of the very low concentration of ^{234}U , most of the alpha particles emitted in the decay of U nuclei come from this particular isotope. From the measured electron distribution, shown in Fig. 5(c), it can be seen that 65% of the detected events can be associated with multielectron events which can be discarded in the analysis of the decay by IC of the isomeric level in ^{235}U . Nevertheless, due to the limited total efficiency of our electron detection set-up, the events in the single electron peak can also be associated with alpha emission. In order to reduce the effect of the background events, we considered an anticoincidence mode of data acquisition between the electron and the alpha particles. The set-up was completed by the addition of alpha-particle detectors mounted as close as possible to the collector without disturbing the collection of electrons as mentioned above.

Four trapezoidal Si 30 μm thick detectors, surrounding the head of the channeltron, detected the alpha particles emitted from the collector in the forward direction. The detection efficiency ϵ_f of these four detectors was measured with calibrated radioactive sources of different diameters and placed at different positions in order to simulate the area of the collector. We measured $\epsilon_f = 0.38 \pm 0.02$ for the detection of alpha particles emitted in the forward direction. Using thin, 2 μm thick, Au collector foils we detected the alpha particles emitted in the backward direction in a thin CsI (TI) scintillator. The crystal had a square shape with a dimension of 29 mm covering the full area of the U layer. The distance between the scintillator and the collector was 2 mm. The scintillation light signal was detected in a photodiode. The characteristics of the photodiode-CsI(TI) assembly for the detection of low-energy alpha particles are given in Ref.

[22]. This detector, scintillator plus photodiode, was moved with the collector from the irradiation chamber to the detection chamber where it was automatically biased. With a 2 μm thick Au collector foil we detect 60% of the particles emitted from the U layer in the direction of the backing. The signals issued from the five particle detectors and the electron detector were recorded in an event-by-event mode in a computerized data acquisition system. Gating conditions have been set on the different parameters in the final analysis of the data. The events showing the detection of an alpha particle were rejected. This condition, added to the selection of the events whose electron pulse heights belong to the peak associated with the multiplicity one, leads to a final reduction of the background events by a factor of 7.5 in comparison with the previous work on the same subject.

In addition to the reduction of the background, the alpha-particle detection presents two important advantages. First, since the alpha detectors are symmetrically mounted with respect to the collector center, any difference in the counting rates in the four forward detectors is an indication of a non-homogeneity of the plasma deposition on the collector. Second, the number of U atoms on the collector can be deduced from the number of detected alpha particles since the detector efficiencies have been carefully measured and because the isotopic composition of the U target and the half-life of each isotope are accurately known. The number of deposited U atoms allows a determination of the thickness of the U layer assuming that all the atoms are at the surface and not implanted into the catcher foil. The thickness and the uniformity of the U layer were checked by measurements of nuclear backscattering using 2 MeV alpha particles from the CENBG Van de Graff accelerator.

As discussed in the appendix, the determination of the thickness of the layer is one of the key issues in the determination of the electron detection efficiency and consequently in the yield of the NEET process. In order to be detected, the electron must first escape from the collector foil. If the U layer on the collector becomes too thick, the IC electron whose maximum energy is of the order of 60 eV, will be stopped inside the layer. The electron mean-free path reaches a minimum value of 5 \AA for an energy around 50 eV [23]. As a consequence, we reduced the thickness of the layer to a value of 25 \AA . This was controlled by the number of laser pulses on the target.

V. EXOELECTRON EMISSION

Emission of low-energy electrons following the deposition of a plasma on a catcher foil has already been reported in the work of Bound and Dyer [10]. This is possibly at the origin of a misleading interpretation of the signal observed in the work of Izawa [6].

Following the definition given by Glaefeke *et al.* [24], exoelectron emission (EE) belongs to the group of emission phenomena which occur during the relaxation of perturbations of the thermodynamic equilibrium in the bulk or at the surface of a solid. Several perturbations can be superimposed. EE occurs spontaneously or as a result of optical or thermal stimulation. For a well-defined perturbation such as

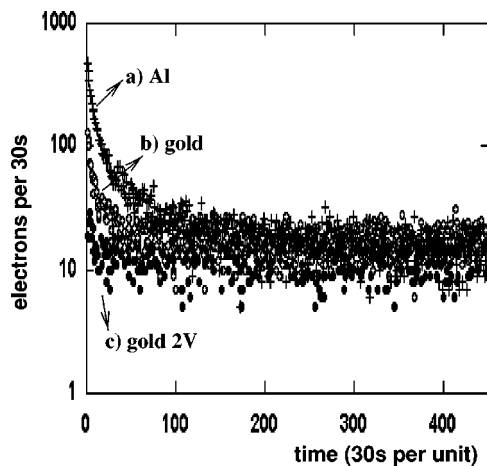


FIG. 6. Number of electrons detected within a time interval of 30 s versus the time elapsed after the end of the plasma collection. The origin of the time on the figure is taken when the collector arrives in front of the electron detector. The time for the collector transfer from the irradiation to the detection chamber is 90 s. Curve a (crosses), the collector is a 50 μm thick pure Al foil; Curve b (open circle): the collector is a thin 2 μm gold foil; Curve c (black dots): same as curve b but the collector foil is biased with 2 V during the detection. The number of laser pulses was equal to 50 and the intensity was $10^{13} \text{ W cm}^{-2}$ in the three cases.

the modification of the surface by adsorption or desorption of clearly identified chemical reactants, bombardment with an electron beam, irradiation with UV or X-ray light, the interpretation of the EE mechanism is already very complex. In the case of the interaction of a solid surface with a plasma the sources of perturbation are multiple. We can identify the bombardment by a very intense beam of free electrons, the bombardment by a beam of low-energy heavy ions, the thermal strength of the surface, the interaction with the reflected laser beam and with the X-rays due to plasma emission. Each of the interaction processes can, by itself, introduce bulk or surface changes in the solid that can give rise to EE. In the following, we only report our results concerning the evolution of EE with the change of some experimental parameters. We focus our attention on the conditions leading to a suppression of EE emission tolerable with the detection of the low-energy electrons emitted in the decay of $^{235}\text{U}^m$. In a first step, we irradiated 50 μm thick gold targets with the laser beam. The beam conditions were the same as the ones used with U targets. The gold plasma was collected on different collectors. Before irradiation, the emission of electrons by the collector was measured. The background level, due to cosmic rays and residual radioactivity was typically 0.5 event per second. After the collection of the plasma, the number of electrons emitted versus the time elapsed from the end of the irradiation was analyzed.

The results obtained with aluminum and gold catchers are reported in Fig. 6. One clearly sees the following:

- 1) Electrons are emitted from all collectors. Since the collected atoms are not radioactive we identify these electrons with exoelectrons.
- 2) The EE emission is larger with the Al catcher than with the Au catcher.

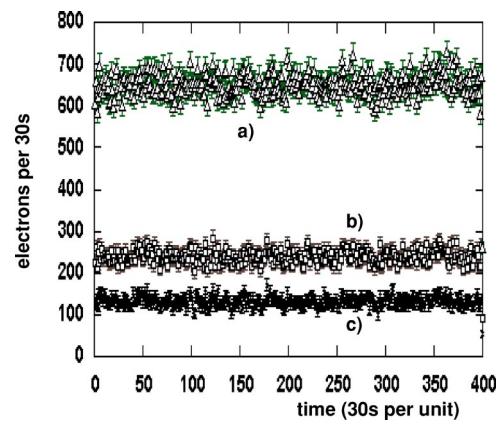


FIG. 7. Electron intensity integrated over 30 s versus the time elapsed after the last laser pulse (a) without condition on the electron PHD; (b) with a gate set on the peak of the electron PHD, (c) same as (b) but an anticoincidence is set between the electron and the alpha-particle signals.

3) The background level is reached after a time longer than the half-life of the ^{235}U isomer.

4) The data cannot be fitted with a simple exponential decay law characterized by a single half-life. They are reproduced by adding two exponential decays with half-lives of the order of 1 mn and 20 mn. For example, fitting curve b with the sum of two exponentials one obtains 2.9 mn and 25.5 mn for the characteristic half-lives and 195 and 40 for the rates of EE detected per 30 s at the end of the irradiation.

In addition, the EE yield increases with the laser intensity. In view of these results, the emission of exoelectrons must be inhibited before one can draw any conclusion about the excitation of the isomeric level based on the detection of IC electrons. Curve b shows the results obtained using a 2 μm thick gold collector. Compared to curve a the EE is strongly reduced in this situation. However, the EE yield changes from foil to foil. We suppose that these changes are correlated with the conditions of the foil surfaces and the variations of the electron work function. Finally, we checked the evolution of the EE emission as a function of an external bias voltage applied to the collector when in the counting position. The EE yield decreased strongly with the application of a positive bias. EE were completely suppressed with a 2 V bias. Curve c in Fig. 6 presents the electron emission as a function of time for a 2 μm thick gold foil catcher biased at 2 V potential during the counting. There is no evidence of EE on this curve. If during the counting the bias potential was removed and the collector grounded, the decay curve characteristic of the EE reappeared. Evidently, the application of a bias voltage on the collector affects also the emission of the IC electrons of $^{235}\text{U}^m$. The total efficiency for electron detection is decreased by 32%.

VI. RESULTS AND DISCUSSION

Each set of measurements was limited to a maximum of 30 consecutive laser pulses to limit the U layer thickness. The distribution of the number of electrons detected, within a time interval of 30 s, is shown in Fig. 7 as a function of the

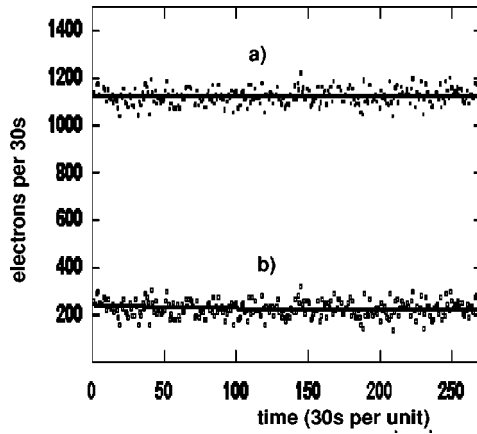


FIG. 8. Number of electrons detected within a time interval of 30 s versus the time elapsed after the end of the plasma collection. The origin of the time on the figure is taken when the collector arrives in front of the electron detector. (a) the distribution corresponds to the sum of 10 independent measurements with selection conditions of Fig. 7(c). (b) a distribution corresponding to Eq. (6) with $m_0=10$ has been added to the experimental distribution shown in (a) after subtraction of a constant value of 900 counts per channel, for viewing purposes. The curve is the result of the fit.

decay time. The origin of the decay time was taken at the end of the last laser pulse. The three curves from top to bottom are obtained considering respectively: (a) the total number of events in the channeltron PHD; (b) the events associated with the peak in the channeltron PHD; (c) events in the peak which are not in coincidence with a signal in one of the alpha-particle detectors. The improvement in the sensitivity for detecting the IC electrons emitted in the decay of the isomer, due to the reduction of the signal associated with the alpha radioactivity of U isotopes and with the emission of exoelectrons is clearly shown in the figure.

Figure 8 presents the summation of ten such measurements (run), performed in identical experimental conditions, with a fresh gold collecting foil at each run. The distribution does not show any signal which can be attributed to the decay of the isomeric state of $^{235}\text{U}^m$. This flat distribution is fully compatible with the emission of delta electrons following the radioactive decay of the U isotopes. It should be noticed that the emission of exoelectrons does not disturb the distribution.

Nevertheless, from this result we can set an upper limit on the excitation rate of the isomeric state in a plasma induced by a laser focussed at an intensity of $10^{13} \text{ W cm}^{-2}$. The minimum number which could have been detected has been determined in the following way. We have added to the curve in Fig. 8 a theoretical distribution of electrons $m_e(t)$ according to the decay of the isomeric state with a half-life of 26.8 min.

$$m_e(t) = m_0 \exp - ((0.5 \ln 2)t/26.8), \quad (6)$$

where t is expressed in unit of 30 s and m_0 is the number of electrons detected in the 30 s after the last laser pulse. The number m_0 was decreased step-by-step. A fit of the distribution shown in Fig. 8(b) was used to obtain the minimum

number m_0 which can be extracted from the data. We find $m_0=10\pm 4$ and a half-life (24 ± 4) mn. From the measurement of the rate of alpha particles detected in the Si detectors we can deduce N_5 the number of U atoms which have been collected:

$$N_5 = (4.6 \pm 0.1) 10^{17} \text{ atoms}. \quad (7)$$

The limit on the *mean* rate of nuclear excitation, $\overline{\lambda_{neet}}$, averaged over the *fwhm* of the laser pulse τ is obtained from the relation

$$m_0 = 30 N_5 \overline{\lambda_{neet}} \tau \lambda_5 \epsilon^T, \quad (8)$$

where $\lambda_5=4.3 \times 10^{-4} \text{ s}^{-1}$ is the deexcitation rate of the isomeric state, $\tau=5 \text{ ns}$ and $\epsilon^T=5 \times 10^{-2}$ is the numerical value of the efficiency of the detection set-up given in the appendix. One obtains

$$\overline{\lambda_{neet}} < 6 \times 10^{-6} \text{ s}^{-1}. \quad (9)$$

The relation Eq. (8) is obtained from Eq. (3) considering a constant excitation rate in the plasma for a time interval of the order of the laser pulse width.

First, we shall successively compare our limit for λ_{neet} with the results obtained in previous experiments [6,9,10]. Second we will discuss this value in relation to theoretical results obtained in [8]. The experimental conditions reported by Izawa *et al.* [6] appear very similar to the ones described in this work. In both cases nanosecond laser pulses are used. In [6], the lower laser intensity, which we estimate to be $10^{11} \text{ W cm}^{-2}$ from the given parameters is compensated by the larger ($\lambda=10 \mu\text{m}$) wavelength of the laser. Assuming that the relation between I , λ , and T in the simplified model holds, one sees that the temperatures reached in the two experiments are of the same order and one therefore expects similar ionization state distributions in the two cases. However, two major differences must be noticed. First, in [6] an electric field was used to separate neutral U atoms from U ions before collecting the plasma. The collection efficiency of the system is not reported, nor was the ratio of neutral to ionized U, so it is difficult to appreciate the improvement due to the charge state separation. Second, in [6], natural U targets were used which only contain 0.7% of ^{235}U . This point severely limits the sensitivity of the experiment. Nevertheless, in spite of this very unfavorable situation, a positive excitation of the isomeric level by the laser was claimed by the authors. Following the reanalysis of the data made in [8], the reported excitation rate was at least $\lambda_{exc}=0.1 \text{ s}^{-1}$ and possibly as high as 2 s^{-1} if a correction for the actual charge state of U ions in the plasma is made. Clearly, such a large signal, which would be 5 orders of magnitude larger than our limit value, could not have been missed in our experiment except in the case of drastically different plasma conditions. On the contrary, we have mentioned above that the conditions for temperature and charge state should be comparable in the two experiments. We are left with the hypothesis of a misinterpretation of the data in [6]. The slow decay component attributed to the decay of the isomer with a lifetime of the order of 26 mn could be, as discussed above, one of the long-lived components in the relaxation of the solid by exoelectron emission.

In the first experiment by Arutyunyan *et al.* [9], a CO₂ laser focussed on UO₂ targets with 6% enrichment in ²³⁵U was used. The laser energy was 5 J and the pulse duration was 200 ns. In [9] no details were given concerning the laser beam focusing, or the number of collected ²³⁵U atoms. The presence or the suppression, if any, of the exoelectrons was not mentioned. In this experiment, the excitation of the isomeric level was not observed although, according to the authors, it was sensitive to a signal with a cross section three orders of magnitude lower than in [6]. This negative result is in agreement with the conclusion of the present paper. However, the lack of experimental details excludes a serious comparison between the two experiments as far as the plasma temperature or the signal-to-background ratio are concerned. In the second experiment, Arutyunyan *et al.* generated a plasma with a high intensity beam of fast electrons. The U atoms blown off the target were collected on a metallic plate and analyzed in a similar way to the previous experiments. They used two types of targets respectively enriched in ²³⁵U at concentrations of 93% and 99.9%. They observed an exponential decay of the delayed electron signal compatible with a half-life of 26 mn with both types of targets. Amazingly, they did not report the presence of EE and they found a larger excitation rate with the targets having a smaller concentration of ²³⁵U which also lead to spectra with a worse signal-to-background ratio. In this experiment, the plasma temperature was estimated to be 20 eV. The excitation rate was $\lambda_{exc} = 3 \times 10^{-5} \text{ s}^{-1}$ in the most favorable case. This value is about the same order as the limit set in the present experiment. Nevertheless, the two results may still be compatible, since in the reanalysis of the data in [8], it was shown that in this experiment, the direct excitation of the isomeric level due to inelastic scattering of the fast electron beam on the U nuclei was the dominant excitation mechanism, larger by two orders of magnitude than NEET or NEEC.

The comparison of our result with the null result reported by Bounds and Dyer [10] is more difficult because of very different experimental conditions in the two cases. In spite of the very careful experimental method followed by the authors, the limit set on the nuclear excitation rate was very high, $\lambda_{exc} = 6 \times 10^7 \text{ s}^{-1}$. The reasons for this high limit are twofold. First, the ionic density of U in the vapor is very low. Second, the excitation time corresponding to the laser pulse duration, less than 1 ps, is very short compared to the ns pulses used in our case. The differences in the coupling between the laser beam and the plasma leads to very different atomic excitation mechanisms. In [10], the ionization of the U atoms resulted from multiphoton absorption from the laser beam. For this reason, the mean value of the charge state distribution was 3⁺ while we expect to reach plasma charge states ranging between 10⁺ and 30⁺ in the present experiment.

In the theoretical work [8] it was shown that in laser-induced plasma experiments, the NEET mechanism is more important than the other possible nuclear excitation mechanisms, NEEC, inelastic electron scattering and photoexcitation. The nuclear excitation rate of the isomeric level was calculated within the assumption of a static model of plasma defined by a single electron temperature and density. The calculations were performed for a single electronic density of

10^{19} cm^{-3} , assuming a constant atomic level width, and two plasma temperatures corresponding respectively to mean U charge states equal to 10⁺ and 23⁺. For ions in the 10⁺ charge state the $6p_{1/2}-5d_{5/2}$ transition energy is nearly resonant with the nuclear transition energy. Nevertheless, due to interaction between the active electron and electrons in the open shells which split the transitions, the energies of the electronic transitions are poorly known. Within a range of $\pm 4 \text{ eV}$ on the energy matching between atomic and nuclear transitions, the calculated excitation rate varies between 10⁻⁹ and 10⁻⁴. For the same reasons, ions in the 23⁺ charge state, would have an excitation rate varying between 10⁻⁶ and 1 in the same uncertainty range. One may think that intermediate plasma temperatures will be associated with λ_{neet} values lying between the two extrema 10⁻⁹ and 1.

In the simplified model with a constant plasma temperature, the lack of signal associated with nuclear excitation is hardly understandable unless the assumptions made in [8] on the widths of the atomic states and on the number of resonances are overestimated. In the more realistic description one sees that the plasma regions in which the conditions for nuclear excitation can be fulfilled is only a small fraction of the plasma volume. In this situation, the theoretical description of the NEET may remain valid but the expression of the experimental limit should be based on the number of U ions in the plasma volume which have encountered the specific temperature and charge state conditions leading to nuclear excitation during a given amount of time. In the present experiment, with a laser intensity of $10^{13} \text{ W cm}^{-2}$, the region of high plasma density located between the target and the coronal absorption region is heated to a temperature of the order of 20 eV where the excitation of the atomic transition $6p_{1/2}-5d_{5/2}$ is expected to be in resonance with the nuclear transition. The temperature and the matter density in this region change very slowly during the duration of the laser pulse so that the resonance condition can be fulfilled during a time interval close to 3 ns as seen in Fig. 2. In this region the results from Morel *et al.* [11] can be compared to our experimental result. For temperatures ranging between 20 eV and 30 eV, an electron density of $5 \times 10^{21} \text{ cm}^{-3}$ the theoretical rate in [11] varies between $3 \times 10^{-6} \text{ s}^{-1}$ and 10^{-5} s^{-1} . If we assume that these plasma conditions are encountered in the plasma during 3 ns as given by the hydrodynamic code then a new limit $\lambda_{neet} = 10^{-5} \text{ s}^{-1}$ is obtained. Clearly this experimental limit is fully compatible with the calculations considering the large difficulties encountered in the determination of the efficiency of the experimental set-up together with the uncertainties in the calculation of the NEET rate in the low temperature-high density domain.

VII. CONCLUSION

We have searched for the excitation of the isomeric level at 76 eV in ²³⁵U in a plasma induced by a laser. At a laser intensity of $10^{13} \text{ W cm}^{-2}$ an upper limit has been set on the nuclear excitation rate $\lambda_{neet} = 6 \times 10^{-6} \text{ s}^{-1}$. The difficulties encountered in this experiment due to exoelectron emission, self-absorption of the low-energy electron in the catcher foil, alpha-particle emission by the radioactive U isotopes have

been quantitatively evaluated. As a result, we have obtained a background signal that is significantly less than that reported in previous experiments on the same subject. One possibility for improving the limit on λ_{neet} is to use targets with a better enrichment in ^{235}U and, more important, a lower concentration in ^{234}U in order to reduce the alpha-emission background. Such an improvement might allow to lower the limit at the needed level for a relevant comparison with the theoretical work by Morel *et al.* In the future, one might also consider increasing the laser intensity to generate the required temperature of 100 eV, in order to achieve the resonance in the dense region where the NEET rate is expected to be larger.

ACKNOWLEDGMENTS

We are grateful to F. Pinard from Aime Coton Laboratory and to F. Leblanc for the long time loan of the laser used in this work. It is a pleasure to acknowledge E. Virassamy-naiken for the production of gold foils. This work was supported in part by the Region Aquitaine.

APPENDIX: DETECTION EFFICIENCY

As shown by Eq. (8) the lower limit set on λ_{neet} strongly depends on the overall probability for detecting the low-energy electrons emitted in the internal conversion decay of the isomeric state. The efficiency ϵ^T is the product of two independent factors. First, a geometrical efficiency ϵ^d defined as the probability of obtaining a signal in the channeltron once the electron is emitted outside from the surface of the collector independent of the electron energy. Second, the probability for the electron emitted at one particular position inside the collector to reach and escape from the collector surface ϵ^e . These two factors can only be estimated on the basis of simulations and partial measurements. Efficiency measurements have been done with the same set-up except that ^{235}U atoms in the isomeric state have been implanted in the collector from a ^{239}Pu source (the alpha decay of ^{239}Pu nuclei populates at 99.9% the isomeric level of ^{235}U). A 239 kBq ^{239}Pu source on a Pt backing was installed in place of the U target. Due to the recoil energy gained in the alpha decay some ^{235}U in the isomeric state were implanted in the collector foil. After 5 min of collection, the collector was transported to a location in front of the electron detector.

The number of electrons n_e recorded per time interval $\delta t=30$ s versus the time elapsed t , is given in Fig. 9. The full line is the result of a fit of the histogram by a decay law

$$n_e = n_0 + n_1 \exp(-0.5t/\tau_2). \quad (\text{A1})$$

The parameters n_0 , n_1 , τ_2 , respectively associated with a constant background, the number of desintegrations at the end of the irradiation and the decay constant τ_2 , in minutes, are free parameters in the fit procedure. The value $\tau_2 = 37.48 \pm 0.08$ mn is in very good agreement with the values found in the literature [15]. Knowing n_1 gives access to the efficiency if the number (N^c) of implanted ^{235}U is known. N^c was determined thanks to a Monte-Carlo simulation of the alpha decay of the Pu nuclei, the recoil of the ^{235}U in the

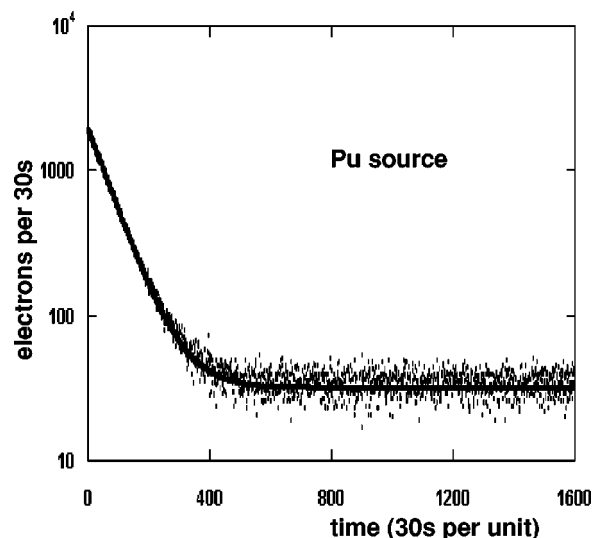


FIG. 9. Number of electrons, from the U^m decay, collected as a function of time using a Pu source. The line is the result of a fit of the data points with Eq. (A1) (see text).

active Pu layer, the backscattering of the U ions at the collector surface, and the source-collector geometry. ϵ^T is obtained from Eq. (A1):

$$n_1 = 1.3 \times 10^{-2} N^c \epsilon^T. \quad (\text{A2})$$

Using a 100 μm Au collector we measured $\epsilon^T = (9.3 \pm 1) 10^{-3}$.

In fact, this value of ϵ^T cannot be used in Eq. (8) because ϵ^e , the probability to escape the collector, is very dependent on the chemical and physical state of the top layers of the collector. If in place of the thick gold foil, the ^{235}U atoms were implanted in a thin 2 μm gold foil, actually used in the experiment, ϵ^T drops to $(5.8 \pm 0.9) 10^{-3}$. This result can be accounted for if a thin oxide layer is introduced on top of the gold surface or if we modify the work function required to escape from the surface. From this result we infer that ϵ^e will change in the realistic situation of an U layer covering the gold surface. In order to check the influence of the U layer on the efficiency we implanted ^{235}U atoms into collectors which had been previously used in the plasma experiments. Thin and thick gold collectors covered by an amount of U varying between 15 and 50 \AA were tested. The value of ϵ^T was $(3.4 \pm 0.1) 10^{-3}$, smaller than the value measured with pure gold foil but independent of the experimental conditions. Another point which should be considered in the determination of the value of ϵ^T to be used in laser plasma experiments concerns the influence of the implantation depths of the U atoms in the collecting foils. Using the program TRIM ([25]), we have simulated stopping of U ions inside gold foils, the U being emitted from the Pu source. The simulation gives a mean stopping range equal to 50 \AA but a large fraction of the range distribution extends above 100 \AA . This range must be compared with the mean-free path of the IC electrons emitted in the decay of ^{235}U nuclei [23]. The effect of the collisions suffered by electrons before escaping from the surface is immediately seen if one implants

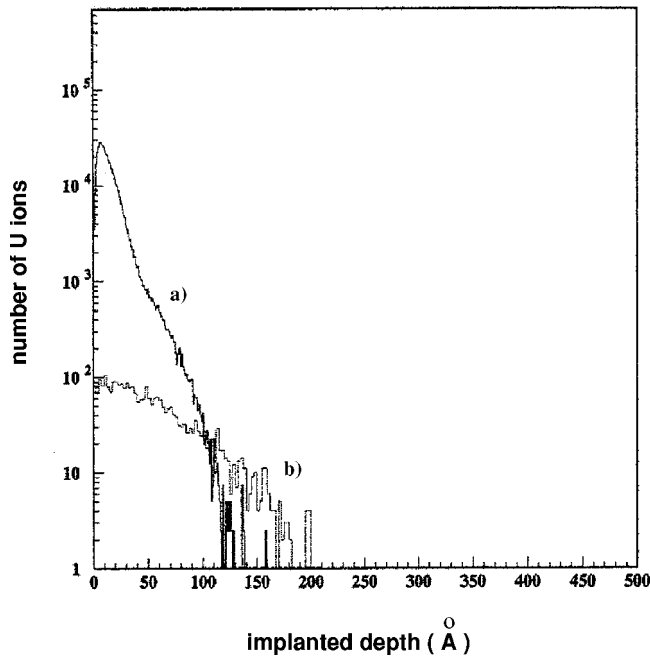


FIG. 10. Results of TRIM calculation for the range distributions of U ions implanted in gold collectors. (a) (heavy line) the ions are accelerated in a plasma induced by laser at $I=10^{13}$ W cm $^{-2}$. (b) (light line) the ions are implanted from a ^{239}Pu source.

^{235}U nuclei in a low Z material such as Al. In this case, the value of ϵ^T decreases down to 4.9×10^{-3} compared to the value $\epsilon^T=9.3 \times 10^{-3}$ found in the gold case. This difference in the value of ϵ^T is well accounted for by the difference in the implantation ranges for the two materials.

In Fig. 10 we have plotted the range distributions in a gold foil of U ions accelerated in the plasma. We considered a Maxwellian energy distribution for the ions with a mean temperature KT equal 400 eV corresponding to the laser intensity 10^{13} W cm $^{-2}$. On the same figure we have also plotted for comparison the U range distribution in the case of the Pu source. With the plasma, the mean range is 11.5 Å and most of the ions are stopped before 40 Å. The difference in the implantation depths between the source and the plasma is likely to induce a large difference in the values of ϵ^T . In

TABLE I. Ranges of U ions and detection efficiency of the experimental set-up versus the nitrogen pressure in the vacuum chamber.

N ₂ pressure (mb)	Collection efficiency (Å)	U mean range	$\epsilon^T 10^{-3}$
10^{-6}	100	50	3.8
1	89	45	8
5	62	30	27
10	23	20	83

order to reach the best agreement in the range distributions for the two situations of U implantation we slowed down the ^{235}U atoms emitted by the Pu source by filling the chamber with nitrogen under different pressures. The TRIM program was used to calculate the implantation efficiency and the range distributions in the gold foil versus the nitrogen pressure. In this measurement we used a 2 μm gold foil covered by a 25 Å U layer deposited by the laser. Then the value of ϵ^T was determined with the fitting procedure as indicated above.

The results in Table I show a drastic change in the detection efficiency with the nitrogen pressure. One sees that for a pressure of 10 mb the mean range of the U ions emitted by the Pu source becomes comparable to the mean range of the implanted U ions accelerated in the plasma under vacuum. The value $\epsilon^T=8.3 \times 10^{-2}$, measured with the Pu source emitting ^{235}U ions in the isomeric state which recoil in N₂ at a pressure of 10 mb and an implant in a thin gold foil covered by a U layer, appears as the best approximation of the detection efficiency. However, the uncertainty on this value is quite large. This uncertainty is mainly due to the use of the TRIM program to calculate the range distributions of implanted U ions. Finally, ϵ^T has to be corrected to take into account the bias voltage of the collector used in order to suppress the emission of exoelectrons. The correction factor is equal to 0.68 as mentioned in the text. Consequently we have adopted a value of $\epsilon^T=5.6 \times 10^{-2}$ for the detection set-up efficiency.

- [1] M. Morita, Prog. Theor. Phys. **49**, 1574 (1973).
 [2] S. Kishimoto *et al.*, Phys. Rev. Lett. **85**, 1831 (2000).
 [3] I. Ahmad *et al.*, Phys. Rev. C **61**, 051304 (2000).
 [4] T. Saito *et al.*, Phys. Lett. **92B**, 293 (1980).
 [5] M. Harston, Nucl. Phys. **A690**, 447 (2001).
 [6] Y. Izawa and C. Yamanaka, Phys. Lett. **88**, 59 (1979).
 [7] V. I. Goldansky and V. A. Namiot, Sov. J. Nucl. Phys. **33**, 169 (1981).
 [8] M. R. Harston and J. F. Chemin, Phys. Rev. C **59**, 2462 (1999).
 [9] R. V. Arutyunyan *et al.*, Sov. J. Nucl. Phys. **53**, 23 (1991).
 [10] J. A. Bounds and P. Dyer, Phys. Rev. C **46**, 852 (1992).
 [11] P. Morel *et al.*, Phys. Rev. A **69**, 063414 (2004).
 [12] F. Attallah *et al.*, Phys. Rev. Lett. **75**, 1715 (1995).
 [13] T. Carreyre *et al.*, Phys. Rev. C **62**, 024311 (2000).
 [14] E. V. Tkalya, Nucl. Phys. **A539**, 209 (1992).
 [15] R. B. Firestone *et al.*, *Table of Isotopes* (Wiley, New York, 1996).
 [16] N. Neve de Nevergnies, Nucl. Instrum. Methods, **109**, 145 (1973).
 [17] D. Colombant and G. F. Tonon, J. Appl. Phys. **44**, 3524 (1973).
 [18] M. Busquet, Phys. Fluids B **5**, 4151 (1993).
 [19] L. Spitzer Jr., *Physics of Fully Ionized Gases* (Wiley, New

- York, 1962).
- [20] N. Neve de Nevergnies and P. Del Marmol, *Phys. Lett.* **49B**, 428 (1974).
- [21] Philips electron multiplier, channeltron model X951.
- [22] J. N. Scheurer *et al.*, *Proceeding of the International Conference on New Nuclear Physic with Advanced Techniques, Greece, June 1991* (World Scientific, London, 1992), p. 108.
- [23] S. Tougaard, *Surf. Interface Anal.* **11**, 453 (1988).
- [24] H. Glaefeke, in *Thermally Stimulated Relaxation in Solids*, edited by P. Braunlich (Springer-Verlag, Berlin, 1979), p. 225.
- [25] J. P. Biersack and L. G. Haggmark, *Nucl. Instrum. Methods* **132**, 647 (1976). Code available TRIM97 from J. Ziegler at IBM, Yorktown Heights <http://www.TRIM.org>.